Available online at www.sciencedirect.com
ScienceDirect
International Journal of Non-Linear Mechanics 42 (2007) 403–410
INTERNATIONAL JOURNAL OF NON-LINEAR MECHANICS
www.elsevier.com/locate/nlm

Non-linear Oberbeck-electroconvection in a poorly conducting fluid through a vertical channel in the presence of an electric field

N. Rudraiah*, Byalakere S. Shashikala

Department of Mathematics, UGC-CAS Centre, Bangalore University, Bangalore, Karnataka, India

Received 4 July 2006; received in revised form 25 November 2006; accepted 21 December 2006

Abstract

Non-linear Oberbeck-electroconvection (OBEC) in a poorly electrically conducting fluid through a vertical channel, when the walls are held at different temperatures with temperature difference perpendicular to gravity, is studied using the modified Navier stokes equation in the presence of both induced and an applied electric field. Both analytical and numerical solutions for the non-linear coupled equations governing the motion are obtained and found that analytical solutions agree well with numerical solutions for values of the buoyancy parameter $N < 1$. It is shown that OBEC can be controlled by maintaining the temperature difference either in the same direction or opposing the potential difference with a suitable value of electric number W. The effect of W on velocity, temperature, rate of heat transfer, skin friction and mass flow rate are computed and the results are depicted graphically. We found that analytical results agree well with numerical results for small values of N. We also found that an increase in W accelerates the flow and hence increases linearly the skin friction and mass flow rate.

Keywords: Oberbeck-electroconvection; Poorly conducting fluid; Electric field; Perturbation technique; Skin friction

1. Introduction

Swift developments in the field of materials science will bring about radical changes in the design of products and their use in modern technologies such as communication and information technology, aviation, automobiles, transportation, production engineering, environmental and nuclear sciences, space and defense, microelectromechanical systems, infrastructure, health and so on. Each of these sectors needs materials which minimize the weight and vibrations and maximize the efficiency. Such materials are changing the way a product is being designed today. It is believed (see [1]) that such suitable materials are smart materials of nanostructure. These along with information technology, biotechnology and cognition technology will improve human performance. At present such smart materials are manufactured using piezoelectric materials. These piezoelectric materials are known to be ideal for ultrasonic applications because of their high frequency response but they may not be of much use for problems involving poorly conducting fluids such as those encountered in biomedical and bioengineering applications because they involve fluids having poor electrical conductivity. Further, for high specific strength the piezoelectric materials exhibit anisotropy and inhomogeneity leading to mathematical complications. Recently, Ng and Rudraiah [2] have shown that these complications can be overcome using smart materials made up of poorly conducting alloys like Nickel–Titanium (N_i–T_i), Aluminum–Nickel (Al–N_i) alloys and so on, as an alternate to piezoelectric smart material. The work of Ng and Rudraiah [2] has been mainly concerned with electroconvection that appears due to solidification of poorly conducting alloys in a horizontal layer cooling form below in the presence of both induced ($\vec{E}_i$) and applied ($\vec{E}_a$) electric fields. The variation of σ with temperature arising due to solidification of poorly conducting alloys by cooling from one side and heating from the other side, releases the free charges resulting in induced electric field, known as thermal electric field $\vec{E}_i$ (see [3–5]). In addition, there may be an applied electric field, $\vec{E}_a$, due to the embedded electrodes of different potentials at the boundaries. The total electric field $\vec{E}(=\vec{E}_i + \vec{E}_a)$, not only produces a current which acts as

* Corresponding author. Tel.: +91 80 22220483; fax: +91 80 22219714.
E-mail address: rudraiahn@hotmail.com (N. Rudraiah).

0020-7462/$ - see front matter © 2007 Elsevier Ltd. All rights reserved.
doi:10.1016/j.ijnonlinmec.2006.12.008

Nomenclature

$\vec{E} = \vec{E}_x, \vec{E}_y$	electric field along x- and y-axis
$\vec{g}$	gravitational acceleration
$\vec{J}$	current density
K	thermal conductivity
N	buoyancy parameter
$\vec{q}$	$(u(y), 0, 0)$ velocity of the fluid
T_1	wall temperature at $y = 1$
T_2	wall temperature at $y = -1$
T_0	temperature of the ambient fluid
q'	rate of heat transfer
b	characteristic length along the flow direction
W_e	electric number
R_e	thermal electric number
ΔT	temperature gradient
Nu	nusselt number
m_E	mass flow rate

Greek symbols

θ	dimensionless temperature
β_T	volumetric expansion for density
υ	kinematic viscosity
ρ	density of the fluid
ρ_e	density of electric charge distribution
σ	electrical conductivity
τ	shearing stress
ϕ	electric potential
α_b	coefficient of volumetric expansion for conductivity
μ	viscosity of fluid
ε_0	electric permittivity
ψ	viscous dissipation

Appendix

a_1	$(W_3 - \alpha^2 W_1)/\alpha^4$ for case 1
a_1	$(W_3 - \alpha^2 W_2)/\alpha^4$ for case 2
c_1	$[\text{Sinh}\,\alpha(RE - W_2) + \alpha^2]/\alpha^2$
c_2	$[\text{Cosh}\,\alpha(RE + W_2)]/\alpha^2$
c_3	$(6a_1\alpha^4\,\text{Sinh}\,\alpha + c_1\alpha^4 - 6RE\,\text{Sinh}\,\alpha)/6\alpha^4$
c_4	$(c_2\alpha^4 - 2a_1\alpha^4\,\text{Cosh}\,\alpha - 2RE\,\text{Cosh}\,\alpha)/2\alpha^4$
a_2	$(c_1c_3 - c_2^2)/12$
a_3	$(2RE - \alpha^2 c_3^2)/2\alpha^2$
a_4	$(-4a_1c_1 - 2a_1c_2\alpha)/\alpha^2$
a_5	$(-6a_1c_1 - 4a_1c_2\alpha + 2a_1c_3\alpha^2)/\alpha^3$
a_6	$(-4REc_1 + 2REc_2\alpha)/\alpha^6$
a_7	$(6REc_1 - 4REc_2\alpha - 2REc_3\alpha^2)/\alpha^7$
a_8	$(4a_1c_1 - a_4\alpha^2)/\alpha^4$
a_9	$(6a_1c_1 - 2a_4\alpha^2 - a_5\alpha^3)/\alpha^5$
a_{10}	$(4REc_1 - a_6\alpha^6)/\alpha^8$
a_{11}	$(-6REc_1 + 2a_6\alpha^6 - a_7\alpha^7)/\alpha^9$
a_{12}	$(2a_1c_1 - a_8\alpha^4)/\alpha^3$
a_{13}	$(-2REc_1 + a_{10}\alpha^8)/\alpha^7$
a_{14}	$a_8 - a_9\alpha$
a_{15}	$a_{10} + a_{11}\alpha$
a_{16}	$-2a_1c_1 - a_4\alpha^2/\alpha$
a_{17}	$2REc_1 + a_6\alpha^6/\alpha^5$
a_{18}	$-a_5\alpha + a_4$
a_{19}	$a_7\alpha + a_6$

sensing, and a force $\rho_e\vec{E}$, which acts as actuator, which are the two properties needed for a material to be a smart material. This force arising in the process of solidifying a poorly conducting alloy, also produces the non-linear Oberbeck-electroconvection (OBEC) instantaneously, due to generation of vortices, by applying a temperature difference perpendicular to gravity. In addition to applications cited above, many geophysical phenomena (see [6]), for example transition between ionosphere and the atmosphere of the earth is a region where electrical forces can dominate in driving the fluid, involve OBEC. This OBEC produces dendrites known as mushy layer, a mixture of solid and fluid, which are considered as impurities in the manufacture of smart materials. Reduction of impurity, arising due to OBEC, requires a mechanism to control OBEC, if not to completely avoid it. This aspect has not been given much attention in the literature in spite of its importance in many problems cited above and the study of it is the main objective of this paper. We try to show that by applying a suitable value of electric potential difference either in a direction opposing or in the same direction of temperature difference it is possible to control OBEC. This requires the nature of velocity and temperature distributions which are obtained both analytically and numerically in this paper.

To achieve the objective of this paper it is planned as follows. The mathematical formulation and the basic equations and the relevant boundary conditions are given in Section 2. The electric potential is obtained in Section 3. The analytical and numerical solutions for velocity and temperature are obtained, in Sections 4 and 5, respectively, when the applied potential difference is either in the same direction or opposing the temperature difference. We note that (see [4,5]) fluids of very low electrical conductivity like Nickel–Titanium (N_i–T_i), Aluminum–Nickel (Al–N_i) alloys, Salt water and so on in the presence of electric field, known as electrohydrodynamics (EHD), permit EHD boundary layer flow separation (see Rudraiah et al. [7]). A considerable amount of research has been devoted to the control of flow separation in ordinary or electrically conducting fluid because it is considered as an undesirable feature, but much attention has not been given to flow separation in EHD. Ordinarily, techniques like suction or injection, blowing and wall movements are used for the control of separation, whereas in EHD considered in this paper an electric field is used to

control flow separation. In this direction the skin friction, the mass flow rate and the rate of heat transfer are useful to understand the control of separation. With this objective, they are discussed in Section 6. These are numerically evaluated and the results obtained from both numerical and analytical methods are compared graphically in the final section and some important conclusions are drawn.

2. Mathematical formulation

The physical configuration considered in this paper is shown in Fig. 1. It consists of an infinite vertical channel bounded on both sides by the rigid isothermal plates embedded with electrodes located at $y = \pm b$ with x-axis in the axial direction and y-axis perpendicular to the plates. In this paper following Rajgopal et al. (see [8]), we consider Oberbeck–Boussinesq, homogeneous, poorly conducting fluid, together with EHD approximations (see Rudraiah et al. [9]), that is σ is very small and hence induced magnetic field is negligible and there is no applied magnetic field. Then the required basic equations for steady flow are the conservation of mass for an Oberbeck–Boussinesq fluid:

$$\nabla.\vec{q} = 0, \tag{2.1a}$$

$$\rho = \rho_0[1 - \beta_T(T - T_0)]. \tag{2.1b}$$

The Navier–Stokes equations are, modified in the sense of addition of electric force $\rho_e\vec{E}$ in the momentum equation.

$$(\vec{q}.\nabla)\vec{q} = -\frac{\nabla p}{\rho_0} + \nu\nabla^2\vec{q} + \frac{\rho\vec{g}}{\rho_0} + \frac{\rho_e\vec{E}}{\rho_0}. \tag{2.2}$$

The energy equation with the addition of ohmic and viscous dissipation is

$$(\vec{q}.\nabla)T = \kappa\nabla^2 T + \frac{\psi}{\rho c_p} + \frac{J^2}{\sigma(\rho c_p)} \tag{2.3}$$

together with the conservation of charges

$$\frac{\partial\rho_e}{\partial t} + (\vec{q}.\nabla)\rho_e + \nabla.\vec{J} = 0 \tag{2.4}$$

and the Maxwell equations for a poorly conducting fluid

$$\nabla.\vec{E} = \frac{\rho_e}{\varepsilon_0}, \tag{2.5a}$$

$$\vec{E} = -\nabla\phi, \tag{2.5b}$$

$$\vec{J} = \sigma\vec{E}, \tag{2.5c}$$

$$\sigma = \sigma_0[1 + \alpha_b(T - T_0)]. \tag{2.5d}$$

In addition to EHD and Oberbeck–Boussinesq approximations, we assume the flow is fully developed and unidirectional in the x-direction, so that the velocity and temperature will be a function of y only. Under these approximations, (2.2)–(2.5), after making them dimensionless using the scales b for length, $\varepsilon_0 V/b^2$ for density of charges, V for potential, V/b for electric field, σ_0 for conductivity, $g\beta b^2(T_1 - T_0)/\nu$ for velocity,

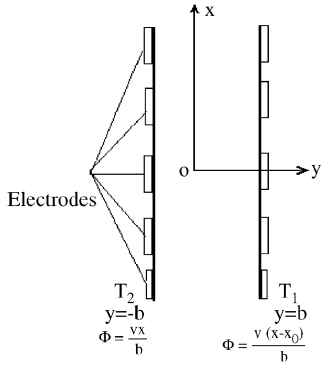

Fig. 1. Physical configuration.

$\Delta T = T_1 - T_0$ for temperature with $\theta = (T - T_0)/\Delta T$, it takes the form

$$\frac{d^2u}{dy^2} + \theta + W_e\rho_e E_x = 0, \tag{2.6}$$

$$\frac{d^2\theta}{dy^2} + N\left(\frac{du}{dy}\right)^2 + R_e\sigma|\vec{E}|^2 = 0, \tag{2.7}$$

$$\sigma(\nabla^2\phi) + \nabla\phi.\nabla\sigma = 0, \tag{2.8}$$

$$\sigma = 1 + \alpha\theta\alpha = \alpha_b\Delta T, \tag{2.9}$$

where $W_e = \varepsilon_0 V^2/\rho_0 g\beta\Delta T b^3$ is the electric number, $N = \rho_0 g^2\beta^2(T_1 - T_0)b^4/K\nu$ the buoyancy parameter and $R_e = \sigma_0 V^2/K\Delta T$ is the thermal electric number.

The required boundary conditions, shown in Fig. 1, to solve the above Eqs. (2.6)–(2.9) after making them dimensionless are

$$u = 0 \quad \text{at } y = \pm 1, \tag{2.10a}$$

$$\theta = 1 \quad \text{at } y = 1, \tag{2.10b}$$

$$\theta = -1 \quad \text{at } y = -1. \tag{2.10c}$$

The solutions of these equations are determined in the subsequent sections both analytically and numerically, using these boundary conditions.

3. Solution for ϕ

The solution for ϕ , according to (2.8) depends on σ which in turn depends on the temperature θ as in (2.9). In a poorly conducting fluid (i.e., $\sigma \ll 1$), the dissipations in (2.7) are negligible and hence σ will depend on the conduction temperature, θ_b, satisfying

$$\frac{d^2\theta_b}{dy^2} = 0. \tag{3.1}$$

The solution of this satisfying the boundary conditions

$$\theta_b = 1 \text{ at } y = 1 \quad \text{and} \quad \theta_b = -1 \text{ at } y = -1 \tag{3.2}$$

is $\theta_b = y$. (3.3)

Then (2.9) becomes

$$\sigma = 1 + \alpha y \approx \mathrm{e}^{\alpha y} \quad (\alpha \ll 1). \tag{3.4}$$

Then (2.8) using (3.4) becomes

$$\frac{\partial^2 \phi}{\partial x^2} + \frac{\partial^2 \phi}{\partial y^2} + \alpha \frac{\partial \phi}{\partial y} = 0. \tag{3.5}$$

To find the solution of (3.5), we considered the following two cases:

Case 1. *The potential difference applied opposite to the temperature difference*: In this case the boundary conditions as shown in Fig. 1, making them dimensionless, are

$$\phi = x \quad \text{at } y = -1 \quad \text{and} \quad \phi = x - x_0 \text{ at } y = 1. \tag{3.6}$$

The solution of (3.5), satisfying (3.6), is

$$\phi = x - \frac{x_0}{2\,\mathrm{Sinh}\,\alpha}(\mathrm{e}^{\alpha} - \mathrm{e}^{-\alpha y}). \tag{3.7}$$

From Eqs. (2.5a)–(2.5d), after making dimensionless using the quantities defined earlier and using (3.7), we get

$$\rho_{\mathrm{e}} = \nabla.\vec{E} = -\nabla^2\phi = -\frac{\alpha^2 x_0 \mathrm{e}^{-\alpha y}}{2\,\mathrm{Sinh}\,\alpha},$$
$$E_x = -1, \quad E_y = \frac{\alpha x_0 \mathrm{e}^{-\alpha y}}{2\,\mathrm{Sinh}\,\alpha}. \tag{3.8}$$

$$\text{Also } \rho_{\mathrm{e}} E_x = \frac{\alpha^2 x_0 \mathrm{e}^{-\alpha y}}{2\,\mathrm{Sinh}\,\alpha}, \quad E_x^2 + E_y^2 = 1 + \frac{x_0^2 \alpha^2 \mathrm{e}^{-2\alpha y}}{4\,\mathrm{Sinh}^2\,\alpha}. \tag{3.9}$$

Case 2. *The potential difference applied in the same direction of temperature difference*: In this case the boundary conditions on ϕ, in dimensionless form, are opposite to those specified in (3.6) and they are

$$\phi_{=} x \text{ at } y = 1 \quad \text{and} \quad \phi = x - x_0 \text{ at } y = -1. \tag{3.10}$$

In this case the solution of (3.5), satisfying (3.10), is

$$\phi = x + \frac{x_0}{2\,\mathrm{Sinh}\,\alpha}(\mathrm{e}^{-\alpha} - \mathrm{e}^{-\alpha y}). \tag{3.11}$$

In this case ρ_{e}, E_y and $\rho_{\mathrm{e}} E_x$ are opposite to those obtained in case 1, whereas E_x and $E_x^2 + E_y^2$ remain the same as in case 1.

Eqs. (2.6) and (2.7) are coupled non-linear equations because of dissipation terms, which are solved both analytically and numerically in the next section.

4. Analytical solutions

Analytical solutions for velocity and temperature are obtained using a regular perturbation technique, with the buoyancy parameter N as the perturbation parameter, which is very small. We look for the solutions of (2.6) and (2.7) in the form

$$u = u_0 + N u_1 + N^2 u_2 + \cdots, \tag{4.1a}$$

$$\theta = \theta_0 + N\theta_1 + N^2\theta_2 + \cdots\ . \tag{4.1b}$$

Here the subscript 0 refers to the solutions for the case in which $N = 0$, which represents physically the solutions in the absence of viscous dissipation and $u_1, u_2, \ldots, \theta_1, \theta_2, \ldots,$, are the perturbation quantities which are assumed to be small compared to u_0 and θ_0.

From Eqs. (2.6) and (2.7), using (3.9), (4.1a) and (4.1b) and equating the coefficients of the like powers of N to zero, we get the following set of equations:

Zeroth order:

$$\text{For case 1: } \frac{\mathrm{d}^2 u_0}{\mathrm{d}y^2} + \theta_0 + W_1 \mathrm{e}^{-\alpha y} = 0. \tag{4.2}$$

$$\text{For case 2: } \frac{\mathrm{d}^2 u_0}{\mathrm{d}y^2} + \theta_0 + W_2 \mathrm{e}^{-\alpha y} = 0, \tag{4.3}$$

$$\frac{\mathrm{d}^2 \theta_0}{\mathrm{d}y^2} + R_{\mathrm{e}} \mathrm{e}^{\alpha y} + W_3 \mathrm{e}^{-\alpha y} = 0. \tag{4.4}$$

First order:

$$\frac{\mathrm{d}^2 u_1}{\mathrm{d}y^2} + \theta_1 = 0, \tag{4.5}$$

$$\frac{\mathrm{d}^2 \theta_1}{\mathrm{d}y^2} + \left(\frac{du_0}{dy}\right)^2 = 0, \tag{4.6}$$

where $W_1 = W_{\mathrm{e}} \alpha^2 x_0 / 2\,\mathrm{Sinh}\,\alpha$ for case 1, $W_2 = -W_{\mathrm{e}} \alpha^2 x_0 / 2\,\mathrm{Sinh}\,\alpha$ for case 2 are the electric numbers, $W_3 = R_{\mathrm{e}} \alpha^2 x_0^2 / 4\,\mathrm{Sinh}^2\,\alpha$ is the thermal electric number. W_{e} is defined earlier.

These equations are solved, using the boundary conditions, in dimensionless form,

$$\theta_0 = 1 \text{ at } y = 1, \quad \theta_0 = -1 \text{ at } y = -1,$$
$$u_0 = u_1 = \theta_1 = 0 \quad \text{at } y = \pm 1. \tag{4.7}$$

Solutions of Eqs. (4.2)–(4.6), satisfying the conditions (4.7), are

$$\theta_0 = y\alpha^2 + R_{\mathrm{e}}(\mathrm{Cosh}\,\alpha - \mathrm{e}^{\alpha y} + y\,\mathrm{Sinh}\,\alpha) + W_2(\mathrm{Cosh}\,\alpha - \mathrm{e}^{-\alpha y} - \mathrm{Sinh}\,\alpha y)/\alpha^2, \tag{4.8}$$

$$u_0 = \frac{R_{\mathrm{e}}}{\alpha^4}(\mathrm{e}^{\alpha y} - \mathrm{Cosh}\,\alpha - y\mathrm{Sinh}\,\alpha) + a_1(\mathrm{e}^{-\alpha y} - \mathrm{Cosh}\,\alpha + y\,\mathrm{Sinh}\,\alpha) + \frac{c_2}{2}(1 - y^2) + \frac{c_1}{6} y(1 - y^2), \tag{4.9}$$

$$\theta_1 = -\frac{R_{\mathrm{e}}^2}{4\alpha^8}\mathrm{e}^{2\alpha y} - \frac{a_1^2}{4}\mathrm{e}^{-2\alpha y} - \frac{c_1^2}{120} y^6 + a_2 y^4 - \frac{c_1 c_2}{20} y^5 + \frac{c_2 c_3}{3} y^3 + a_3 y^2 - \frac{c_1 a_1}{\alpha} y^2 \mathrm{e}^{-\alpha y} + a_4 y \mathrm{e}^{-\alpha y} + a_5 \mathrm{e}^{-\alpha y} + \frac{c_1 R_{\mathrm{e}}}{\alpha^5} y^2 \mathrm{e}^{\alpha y} + a_6 y \mathrm{e}^{\alpha y} + a_7 \mathrm{e}^{\alpha y} - \frac{p_1}{2}(1 + y) - \frac{p_2}{2}(1 - y), \tag{4.10}$$

$$u_1 = \frac{R_e^2}{16\alpha^{10}}e^{2\alpha y} + \frac{a_1^2}{16\alpha^2}e^{-2\alpha y} + \frac{c_1^2}{6720}y^8 + \frac{c_1c_2}{840}y^7 - \frac{a_2}{30}y^6 - \frac{c_3c_2}{60}y^5 - \frac{a_3}{12}y^4 + \frac{a_1c_1}{\alpha^3}y^2e^{-\alpha y} + a_8ye^{-\alpha y} + a_9e^{-\alpha y} - \frac{R_ec_1}{\alpha^7}y^2e^{\alpha y} + a_{10}ye^{\alpha y} + a_{11}e^{\alpha y} + \frac{p_1}{4}y^2\left(\frac{3+y}{3}\right) + \frac{p_2}{4}y^2\left(\frac{3-y}{3}\right) - \frac{p_4}{2}(1-y) - \frac{p_3}{2}(1+y). \quad (4.11)$$

The velocity (u) and temperature (θ), can be obtained, respectively, using (4.1a), (4.1b) and (4.2)–(4.6). We note that a_1, given in the Appendix, involves W_1 for case 1 and W_2 for case 2. These u and θ are computed for the cases 1 and 2 and the results are compared with the numerical solution obtained in the next section.

5. Numerical solutions

The analytical solutions obtained in Section 4 using regular perturbation technique are valid only for small values of buoyancy parameter N. However, in many practical problems like unconventional generators, shock tubes, nuclear reactors and so on, the values of N are usually large and regular perturbation solutions cannot be used. For arbitrary values of N, analytical solutions for non-linear coupled equations (2.6) and (2.7) are complicated and hence we resort to numerical solution, using a finite difference technique. The velocity and energy equations are solved using the central difference method. The use of central difference scheme replaces the derivative with corresponding central difference approximations leading to a set of linear algebraic equations. The solution of reduced algebraic equations are obtained by the method of Successive Over Relaxation (SOR). The relaxation parameter ω is fixed by comparing the numerical results with those obtained by analytical method. The convergence criterion is based on the step size and the previous iterations for the iterative difference to the order 10^{-6}.

The finite difference equations equivalent to Eqs. (2.6) and (2.7) with 21 mesh points with the step size 0.1 are

$$\frac{u_{j-1} - 2u_j + u_{j+1}}{(\Delta y)^2} + W_1e^{-\alpha y_j} + \theta_j = 0.$$

Solving for u_j,

$$u_j = \tfrac{1}{2}[u_{j-1} + u_{j+1} + W_1e^{-\alpha y_j}(\Delta y)^2 + \theta_j(\Delta y)^2], \quad (5.1)$$

$$\frac{\theta_{j-1} - 2\theta_j + \theta_{j+1}}{(\Delta y)^2} + N\left(\frac{u_{j+1} - u_{j-1}}{2\Delta y}\right)^2 + R_ee^{\alpha y_j} + W_3e^{-\alpha y_j} = 0.$$

Solving for θ_j,

$$\theta_j = \frac{1}{2}\left[\begin{matrix}\theta_{j-1} * (\Delta y)^2 + \theta_{j+1} * (\Delta y)^2 + \frac{N}{4}(u_{j+1} - u_{j-1})^2 \\ +R_e * (\Delta y)^2 * e^{\alpha y_j} + W_3 * (\Delta y)^2 * e^{-\alpha y_j}\end{matrix}\right]. \quad (5.2)$$

Applying SOR, we obtain from Eqs. (5.1) and (5.2),

$$U(J) = \frac{\omega}{2}[U(J-1)+U(J+1) + W_1 * (\Delta y)^2 * \mathrm{Exp}(-\alpha y_j) + \theta I(J) * (\Delta y)^2] + (1-\omega)UI(J). \quad (5.3)$$

$$\theta(J) = \frac{\omega}{2}\left[\begin{matrix}\theta(J-1)+\theta(J+1)+\frac{N}{4(\Delta y)^2} \\ \quad \times (UI(J+1) - U(J-1))^2 + R_e * \mathrm{Exp}(\alpha y_j) \\ +W_3 * \mathrm{Exp}(-\alpha y_j)\end{matrix}\right] + (1-\omega)\theta I(J). \quad (5.4)$$

In (5.3) and (5.4), ω is the relaxation parameter. The value of ω is fixed at 1.645 after checking the closeness with analytical solutions. The solutions (5.1) and (5.2) are computed for different values of the parameters and the results are depicted graphically along with the analytical results and conclusions are drawn in the final section.

6. Skin friction, rate of heat transfer and mass flow rate

In many practical applications involving separation of flow it is an advantage for us to know the skin friction and the rate of heat transfer at the boundaries. These can be determined once we know the velocity and temperature distributions. The skin friction τ at the walls is defined as

$$\tau' = \mu(\partial u/\partial y)_{y=\pm b}. \quad (6.1)$$

Making this dimensionless, using the scale $\rho g\beta_T b\Delta T$ for τ and using the scales for u and y used earlier, we get

$$\tau = (\mathrm{d}u/\mathrm{d}y)_{y=\pm 1}. \quad (6.2)$$

This, using (4.1a), takes the form

$$\tau = (\mathrm{d}u_0/\mathrm{d}y)_{y=\pm 1} + N(\mathrm{d}u_1/\mathrm{d}y)_{y=\pm 1}. \quad (6.3)$$

Here $(\mathrm{d}u_0/\mathrm{d}y)$ and $(\mathrm{d}u_1/\mathrm{d}y)$ can be obtained using the analytical solutions given by (4.9) and (4.11). Eq. (6.2) is also computed numerically using the finite difference scheme as explained in Section 5.

Similarly, the rate of heat transfer between the fluid and the plate is given by the heat flux

$$q' = -K(\partial T/\partial y)_{y=\pm b}. \quad (6.4)$$

This, using the scale $K\Delta T$ for the heat flux, is expressed in terms of the Nusselt number, Nu, given by

$$Nu = (\mathrm{d}\theta/\mathrm{d}y)_{y=\pm 1}. \quad (6.5)$$

This Nu, using (4.1b), takes the form

$$Nu = (\mathrm{d}\theta_0/\mathrm{d}y)_{y=\pm 1} + N(\mathrm{d}\theta_1/\mathrm{d}y)_{y=\pm 1}, \quad (6.6)$$

where $(\mathrm{d}\theta_0/\mathrm{d}y)$ and $(\mathrm{d}\theta_1/\mathrm{d}y)$ can be computed using the analytical solution given by (4.8) and (4.10). This Nu, given by (6.5), is also numerically evaluated using the finite difference scheme as explained in Section 5.

The skin friction and the rate of heat transfer given above are computed for different values of N and the results obtained

from analytical and numerical techniques are compared graphically and suitable conclusions are drawn in the final section.

If m_E denotes the mass flow rate per unit channel width in the presence of dissipation, then

$$m_E = \int_{-b}^{b} \rho_0 u \, \mathrm{d}y. \tag{6.7}$$

It is of practical interest to find the mass flow rate given by (6.7) using both analytical and numerical techniques explained in Sections 4 and 5, respectively. The results so obtained are discussed in the final section.

7. Results and discussion

The effect of electric field on the velocity, temperature, skin friction, rate of heat transfer and mass flow rate are obtained both analytically and numerically. The analytical solutions are obtained from regular perturbation technique valid for small values of N ($\approx 10^{-1}$). To obtain the results for arbitrary values of N, the solutions of coupled non-linear differential equations are obtained numerically using central difference scheme. The system of algebraic equations resulting from the use of central differencing are solved using the successive over relaxation method.

The analytical solutions are computed for different values of W_e, R_e and N and the results are compared in Figs. 2–8 with those obtained from the numerical technique.

Figs. 2 and 3, are concerned with velocity distributions in the presence of the dissipative effects for various values of electric number (W_e) and the buoyancy parameter (N). Similarly Figs. 4 and 5 are concerned with temperature distributions in the presence of dissipative effects for different values of thermal electric number (R_e) and the buoyancy parameter.

From Figs. 2 and 3, we found that the analytical solutions are in good agreement with the numerical results up to $N = 1$ and

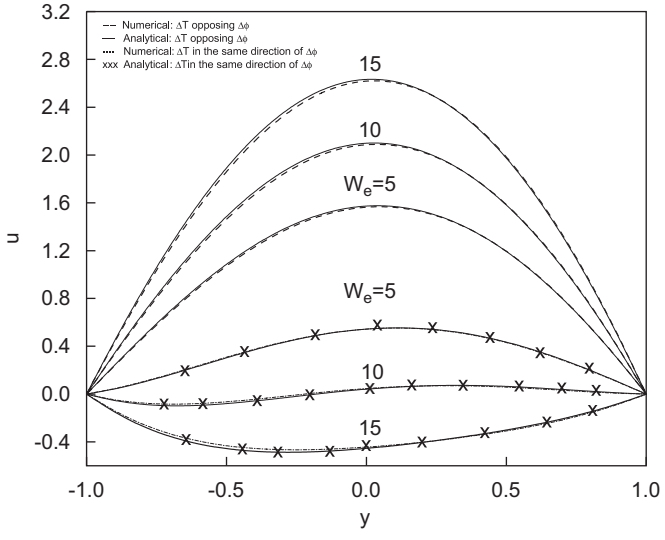

Fig. 2. Velocity profiles for different values of W_e with $N = 0.1$, $R_e = 1$, $\alpha = 0.1$, $X_0 = 4$.

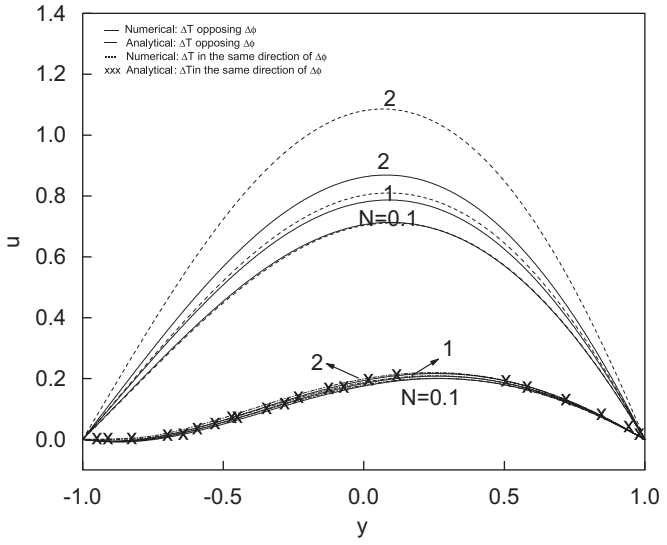

Fig. 3. Velocity profiles for different values of N with $W_e = 5$, $R_e = 1$, $\alpha = 0.1$, $X_0 = 4$.

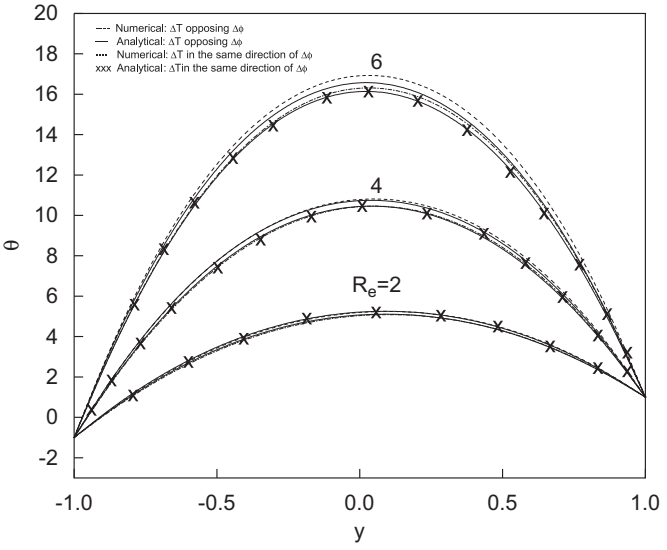

Fig. 4. Temperature profiles for different values of R_e with $N = 0.1$, $W_e = 5$, $\alpha = 0.1$, $X_0 = 4$.

they deviate considerably for $N > 1$. We also observe that for both cases 1 and 2, the velocity and temperature distributions, increase with an increase in (W_e), (R_e) and N.

In particular, we found that, an increase in electric field accelerates the flow more when ΔT opposes $\Delta\phi$ compared to the case when ΔT and $\Delta\phi$ are in the same direction. This can be effectively used in many industrial problems, particularly in lubrication and in electrical transformers, for effective cooling of the machineries, choosing a suitable value of N. Further, we also note that, the flow reversal occurs for higher values of N when the temperature difference ΔT is in the same direction of potential difference $\Delta\phi$. However, this flow reversal disappears when the temperature difference opposes the potential difference.

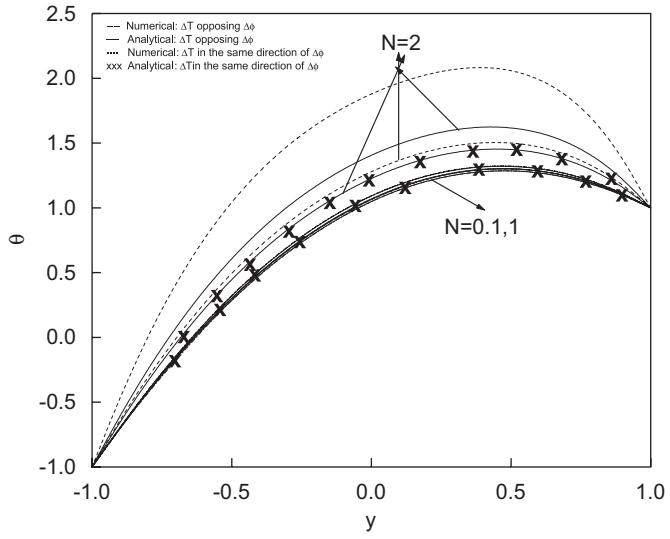

Fig. 5. Temperature profiles for different values of N with $R_e = 1$, $W_e = 5$, $\alpha = 0.1$, $X_0 = 4$.

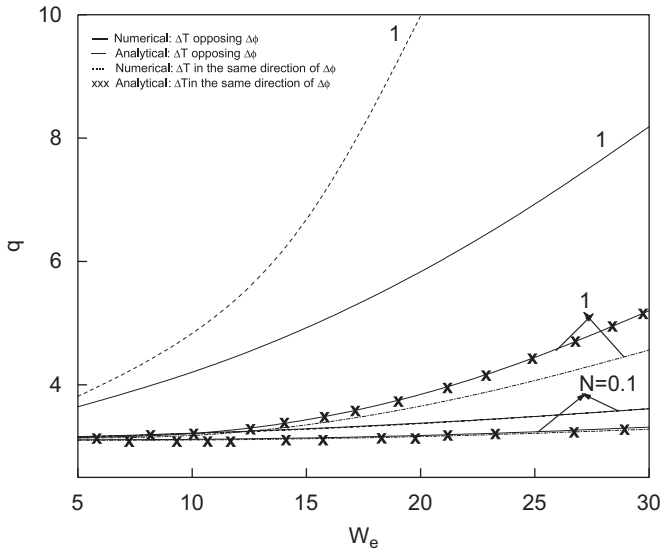

Fig. 7. Rate of heat transfer for different values of N with $R_e = 1$, $W_e = 5$, $\alpha = 0.1$, $X_0 = 2.1$.

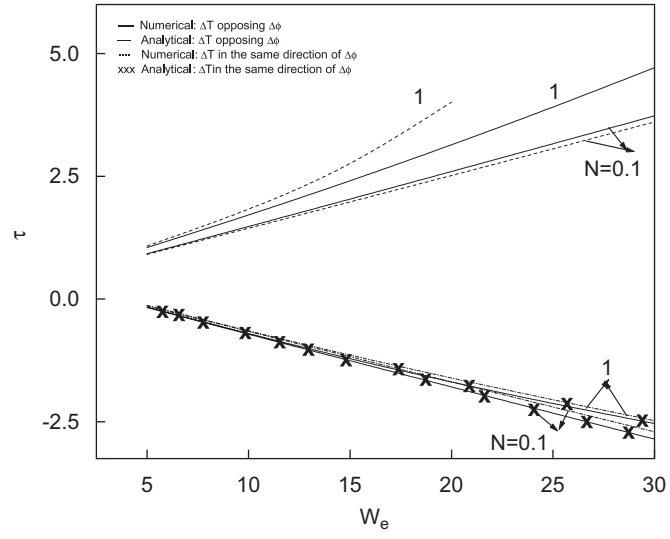

Fig. 6. Skin friction for different values of N with $R_e = 1$, $W_e = 5$, $\alpha = 0.1$, $X_0 = 2.1$.

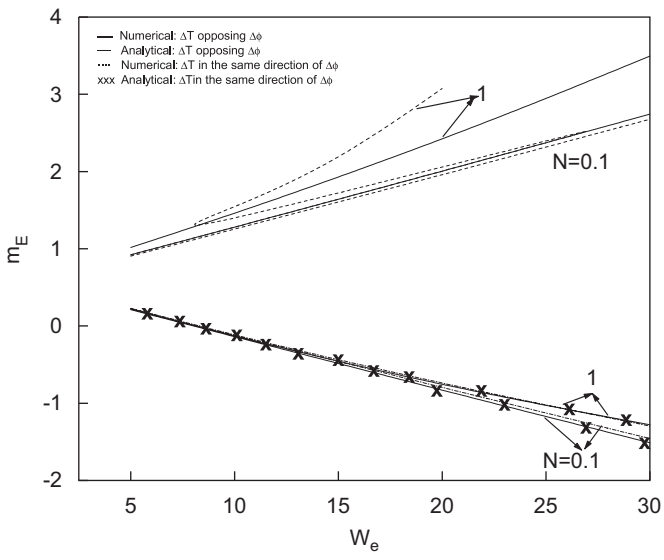

Fig. 8. Mass flow rate for different values of N with $R_e = 1$, $W_e = 5$, $\alpha = 0.1$, $X_0 = 2.1$.

The skin friction, rate of heat transfer and mass flow rate obtained analytically are computed in the presence of dissipative effects for different values of N and the results obtained from both analytical and numerical procedures are in Figs. 6–8. From these, we found that they increase with an increase in N because as N increases, the temperature difference also increases, resulting in a large convection which transfers more heat.

Finally we conclude that with a proper choice of external constraints of electric field and the temperature difference it is possible to control OBEC, which is useful in the manufacture of new materials like smart materials free from impurities.

Acknowledgments

This work is supported by UGC under CAS in fluid mechanics of SAP. The work of N.R is also supported by DST under the project SR/S4/AS-237/04. One of us (S.B.S) is indebted to UGC-CAS for providing her a Junior Assistant Fellowship leading to Ph.D. under SAP.

References

[1] N. Rudraiah, Modeling of Nano and Smart Materials, Book paradise, India, 2003.

[2] N. Rudraiah, C.O. Ng, A model for manufacture of nano-sized smart materials free from impurities, Curr. Sci. 86 (8) (2004) 1076 (review articles).
[3] C.O. Lee, M.U. Kim, D.I. Kim, Electro hydrodynamic cellular bulk convection induced by a temperature gradient, Phys. Fluids 15 (1972) 789.
[4] R.J. Turnbull, Electroconvective instability with a stabilizing temperature gradient-I theory, Phys. Fluids 11 (12) (1968) 2588.
[5] R.J. Turnbull, Free convection from a heater vertical plate in a direct-current electric field, Phys. Fluids 12 (11) (1969) 2255.
[6] W.V.R. Malkus, G. Veronis, Surface electroconvection, Phys. Fluids 4 (1) (1961) 13.
[7] N. Rudraiah, T. Masuoka, P. Nair, Effect of combined Brinkman and electro boundary layer on the onset of Marangoni electroconvection in a poorly conducting fluid-saturated porous layer cooled form below in the presence of an electric field, J. Porous Media 10 (5) (2007), to appear.
[8] K.R. Rajgopal, et al., On the Oberbeck–Boussinesq approximation, in: Mathematical Models and Methods in Applied Sciences, vol. 6, No. 8, 1996, pp. 1157–1167.
[9] N. Rudraiah, B.S. Krishnamurthy, R.D. Mathad, The effect of oblique magnetic field on the surface instability of a finite conducting fluid layer, Acta Mech. 119 (1996) 165.